Available online at www.derpharmachemica.com

ISSN 0975-413X
CODEN (USA): PCHHAX

Der Pharma Chemica, 2016, 8(10):179-186
(http://derpharmachemica.com/archive.html)

3-Allyl-6-bromo-2-(4-methoxyphenyl)-*3H*-imidazo[4,5-b]pyridine as a potential inhibitor for Corrosion of mild steel in in 1.0 HCl solution

S. Bourichi[1], Y. Kandri Rodi[1], H. Elmsellem[2], H. Steli[5], Y. Ouzidan[1], N. K. Sebbar[3], F. Ouazzani Chahdi[1], E. M. Essassi[3], F. El-Hajjaji[4] and B. Hammouti[2]

[1]Laboratory of Applied Organic Chemistry, Faculty of Science and Technology, University Sidi Mohammed Ben Abdallah, Fez, Morocco
[2]Laboratoire de chimie analytique appliquée, matériaux et environnement (LC2AME), Faculté des Sciences, B.P. 717, 60000 Oujda, Morocco
[3]Laboratoire de Chimie Organique Hétérocyclique, URAC 21, Pôle de Compétences Pharmacochimie, Mohammed V University, Faculté des Sciences, Av. Ibn Battouta, BP 1014 Rabat, Morocco
[4]Laboratoire d'Ingénierie d'Electrochimie, Modélisation et d'Environnement (LIEME), Faculté des sciences/Université Sidi Mohammed Ben Abdellah, Fès, Maroc
[5]Laboratoire mécanique & énergétique, Faculté des Sciences, Université Mohammed Premier, Oujda, Maroc

---

ABSTRACT

The inhibitory effect of 3-allyl-6-bromo-2-(4-methoxyphenyl)-3H-imidazo[4,5-b]pyridine (P2) on corrosion of mild steel in aqueous 1 M HCl was investigated by weight loss method, potentiodynamic polarisation technique and electrochemical impedance spectroscopy (EIS). The inhibition efficiency of P2 on corrosion of mild steel in 1 M HCl solution increases on increasing in concentration of the P2. Potentiodynamic Polarization measurement indicates that P2 acts as a mixed-type inhibitor. The nature of adsorption of the P2 on mild steel surface is found to obey Langmuir adsorption isotherm. EIS measurement result is also correlated with the result of polarization. DFT study confirmed the adsorption of inhibitor molecules on mild steel surface.

Keywords: Mild steel; Acid corrosion; EIS ; Corrosion inhibition ; DFT.

INTRODUCTION

Corrosion processes are responsible for numerous losses mainly in the industrial scope. Prevention is the best way to combat corrosion. The corrosion inhibitor is one of the best known methods of corrosion protection and one of the most useful on the industry. This method is following stand up due to low cost and practice method [1-4]. There are various corrosion inhibitors; the most used are organic inhibitors acting by adsorption. Some organic compounds have also been used as inhibitors of steel corrosion in 1.0 M HCl solution [5-8], such as pyrazoles [9], triazoles [10], tetrazoles [11], imidazole derivatives [12], and imidazopyridine [13]. In the present paper, an imidazopyridine derivative newly synthesized was tested as corrosion inhibitor for mild steel in 1.0 M HCl using potentiodynamic polarization methods and electrochemical impedance spectroscopy (EIS) measurements and gravimetric method (**Scheme 1**).

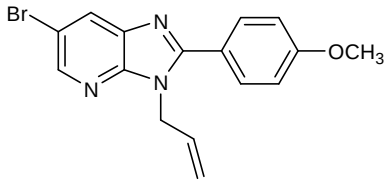

Scheme 1: 3-allyl-6-bromo-2-(4-methoxyphenyl)-3H-imidazo[4,5-b]pyridine(P2)

MATERIALS AND METHODS

2.1. Synthesis of inhibitor

The structure of the studied imidazopyridine derivative is given in scheme1. The chemical synthesis procedure is: The mixture of 0,2g (0,65mmol) of 6-bromo-2-(4 methoxyphenyl)-3*H*-imidazo[4,5-b]pyridine dissolved in 25ml of DMF, and potassium carbonate K_2CO_3 0,12g (0,92mmol) was stirred magnetically hang for 5 minutes and then added 0.06g (0,19mmol) of tetra-n-butylammonium bromide (TBAB) and 1,2 equivalent of allyl bromide. Stirring was continued at room temperature for 6 hours. After removing salts by filtration, the DMF was evaporated under reduced pressure and the residue obtained is dissolved in dichloromethane. The remaining salts are extracted with distilled water and the resulting mixture was chromatographed on silica gel column (eluent: ethyl acetate/hexane (1/3)). The product was obtained with 45 % yield.

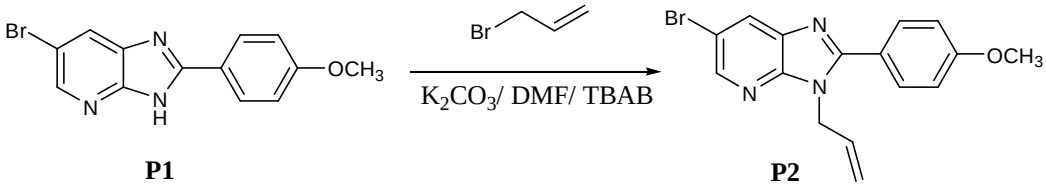

P1 **P2**

Scheme 2: Synthesis of 3-allyl-6-bromo-2-(4-methoxyphenyl)-3H-imidazo[4,5-b]pyridine (P2)

The analytical and spectroscopic data are conforming to the structure of compounds formed:

(P2): Yield: 45%**; MP =** 450-452**K; NMR^{1}H ($CDCl_3$; 300MHz) δ ppm:** 8.43(d,1H,H_{py},J=2.1Hz) ; 8.19(d,1H,H_{py},J=2.1Hz) ;7.81-7.78(m,2H,H_{Ar}) ;7.07-7.04(m,2H,$H_{Ar)}$; 6.06-6.19 (m, 1H, CH); 5.28-5.32 (d, 2H, CH_2, J= 0.9); 4.96- 4.99 (m, 2H, CH_2); 3.90 (s, 3H, $OCH_{3)}$. **NMR^{13}C ($CDCl_3$; 300MHz) δ ppm**: 161.53, 155.93, 147.44, 136.34, 121.74, 114.11 (C_q); 144.34, 130.62, 128.45, 114.35(CH_{Ar}); 132.52 (CH); 117.36; 45.80 (CH_2); 55.43 (OCH_3).

RESULTS AND DISCUSSION

3.1 Weight Loss Measurements

The weight loss data made primarily at 6 hours of immersion at room temperature (308 K) were given in Table 1, where the inhibition efficiency was calculated using the following equation (1):

$$V0 \text{ X } 10 \qquad \textbf{(1)}$$

Where V_0 and V are the values of corrosion rate without and with inhibitor, respectively.

The fractional surface coverage θ can be easily determined from the weight loss measurements by the ratio Ew (%)/100, where Ew (%) is inhibition efficiency and calculated using Relation (1). The data obtained suggest that the P2 get adsorbed on the mild steel surface at studied temperature and corrosion rates increased in presence of inhibitor in 1 M HCl solutions.

Table 1. Corrosion rate and inhibition efficiency in the absence and presence of P2 in 1 M HCl solution at 308K

Inhibitor	Concentration (M)	*v* ($mg.cm^{-2}h^{-1}$)	Ew (%)
HCl	**1**	0.82	--
P2	$\mathbf{10^{-6}}$	0.09	89
	$\mathbf{10^{-5}}$	0.22	73
	$\mathbf{10^{-4}}$	0.41	50
	$\mathbf{10^{-3}}$	0.53	35

Table 1 indicates that the corrosion rate of mild steel decreased on increasing concentration. This behavior could be attributed to the increase in adsorption of P2 at the mild steel/solution interface on increasing its concentration.

3.2. Adsorption isotherm

The mechanism of the interaction between inhibitor and the electrode surface can be explained using adsorption isotherms. Several adsorption isotherms were tested and the Langmuir adsorption isotherm was found to provide best description of the adsorption behavior of the investigated inhibitor. The Langmuir isotherm is given by the equation [14-15]:

$$\frac{C}{\theta} = \frac{1}{k} + C \quad \textbf{(2)}$$

With $\Delta G_{ads} = -RT\ln(55{,}5K)$ **(3)**

Where C_{inh} is the concentration of inhibitor, K the adsorptive equilibrium constant, ΔG_{ads} is the standard free energy of adsorption reaction, R is the universal gas constant, T is the absolute temperature in Kelvin, θ is the fraction of the surface covered calculated as follows θ = Ew(%)/100 and the value of 55.5 is the concentration of water in the solution in mol/L.

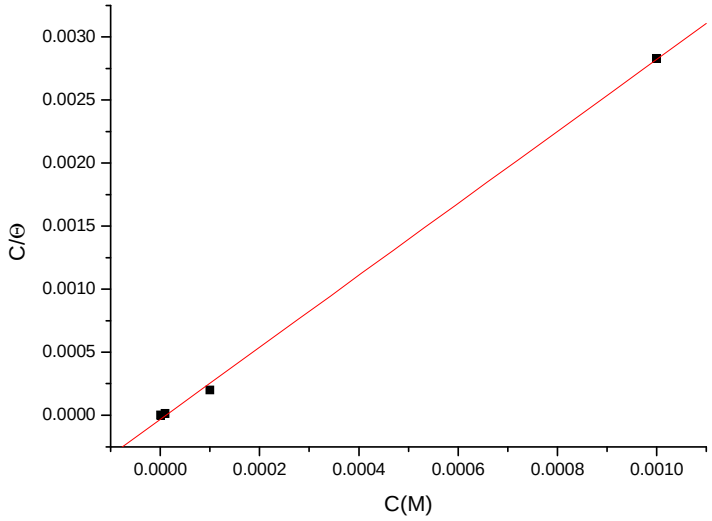

Figure 1: Langmuir adsorption plot of mild steel in 1 M HCl solution containing various concentrations of P2

Figure 1 shows the dependence of the ratio C_{inh}/θ as function of C_{inh}. Linear plot is obtained with slope and correlation coefficient close to 1.

3.3. Electrochemical impedance spectroscopy (EIS)

The electrochemical impedance spectroscopy (EIS) measurements are carried out with the electrochemical system, which included a digital potentiostat model Voltalab PGZ100 computer at Ecorr after immersion in solution without bubbling. After the determination of steady-state current at a corrosion potential, sine wave voltage (10 mV) peak to peak, at frequencies between 100 kHz and 10 mHz are superimposed on the rest potential. Computer programs automatically controlled the measurements performed at rest potentials after 30 min of exposure at 308 K. The impedance diagrams are given in the Nyquist representation. Inhibition efficiency (E_R%) is estimated using the equation 4, where $R_t(0)$ and Rt(inh) are the charge transfer resistance values in the absence and presence of inhibitor, respectively:

$$E_R\% = (R_{t(inh)} - R_{t(0)} / R_{t(inh)})*100 \quad \textbf{(4)}$$

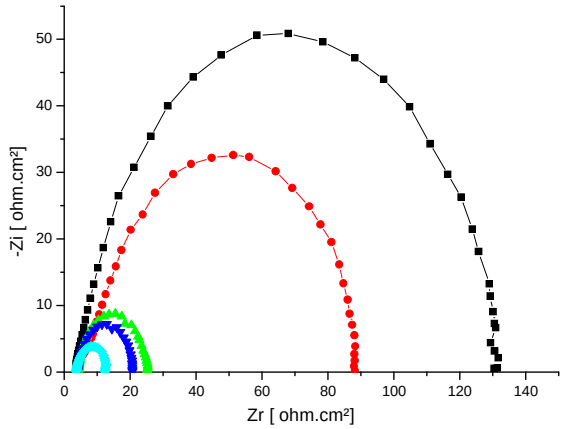

Figure 2: Nyquist plots of the corrosion of mild steel in 1 M HCl without and with different concentrations of P2 at 308K

Table 2. ***Impedance parameters of mild steel in*** **1 M HCl** ***containing different concentrations of P2***

Inhibitor	Concentration (M)	R_{ct} (Ω cm^2)	C_{dl} (µf/cm^2)	E (%)
HCl	**1**	15	200	--
P2	$\mathbf{10^{-6}}$	19	163	21
	$\mathbf{10^{-5}}$	25	121	40
	$\mathbf{10^{-4}}$	83	69	82
	$\mathbf{10^{-3}}$	129	56	**88**

The impedance data listed in the table 2 indicate that the values of both Rct and E% are found to increase by increasing the inhibitor concentration, while the values of Cdl are found to decrease. This behavior can be attributed to a decrease in dielectric constant and/ or an increase in the thickness of the electric double layer, suggesting that the inhibitor molecules act by adsorption mechanism at mild steel/acid interface [17-18].

3.4. Potentiodynamic Polarization measurement

Potentiodynamic polarization curves for mild steel in 1 M HCl solutions in the absence and presence of various concentrations of P2 at 308 K are shown in figure 3. The extrapolation of Tafel straight line allows the calculation of the corrosion current density (icorr). The values of icorr, the corrosion potential (Ecorr), cathodic Tafel slopes (βc) and the percentage of inhibition efficiency (Ep%) are given in the table 3.

Inhibition efficiency (Ep%) is defined as Equation 4, where $i_{corr(0)}$ and $i_{corr(inh)}$ represent corrosion current density values without and with inhibitor, respectively.

$$E_p\% = (i_{corr(0)} - i_{corr(inh)} / i_{corr(0)})*100 \quad \textbf{(5)}$$

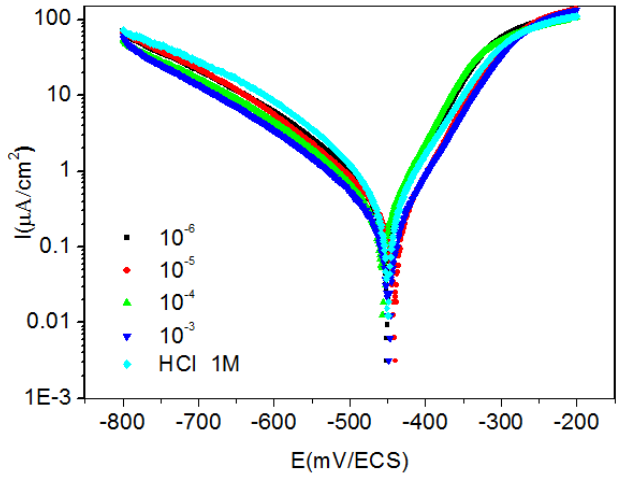

Figure 3. Potentiodynamic polarization curves for mild steel in 1 M HCl solution in absence and presence of different concentrations of P2 at 308 K

Table 3. Polarization parameters and corresponding inhibition efficiency for the corrosion of the mild steel in 1 M HCl without and with addition of various concentrations of P2 at 308k

Inhibitor	Concentration (M)	$-E_{cor}$ (mV)	β_C (V/dec)	I_{cor} ($\mu A/cm^2$)	Ep (%)
HCl	**1**	439	0,13	1195	-
P2	10^{-6}	461	0,15	530	55
	10^{-5}	442	0,12	365	68
	10^{-4}	437	0,10	346	72
	10^{-3}	449	0,18	277	78

Inspections of the data of the figure 3 infer that, at a given temperature 308K, the addition of the P2 to the acid solution increases both the anodic and cathodic overpotentials, decreases the corrosion current density (icorr). The change in cathodic slopes (βc) shown in the table 3 indicates that adsorption of P2 on mild steel modify the mechanism of the anodic dissolution as well as cathodic hydrogen evolution. From figure 3, it is cleared that both cathodic and anodic reactions are inhibited but the cathodic reaction (Hydrogen evolution reaction) is seem to be slightly more inhibited. From table 3, it is also cleared that the inhibition increases with increase in concentration and there is no definite trend in the shift of Ecorr values in presence of various concentration of P2 in 1 M HCl solutions. This result indicates that P2 may be classified as a mixed type of inhibitor in 1 M HCl solution [19].

3.5. Quantum chemical calculations

Quantum chemical calculations are used to correlate experimental data for inhibitors obtained from different techniques (viz., electrochemical and weight loss) and their structural and electronic properties. According to Koop man's the orem [20], E_{HOMO} and E_{LUMO} of the inhibitor molecule are related to the ionization potential (I) and the electron affinity (A), respectively. The absolute electronegativity (χ) and global hardness (η) of the inhibitor molecule are approximated as follows [21]:

$$\chi = \frac{I+A}{2}\ ,\quad \chi = -\frac{1}{2}(E_{HOMO} + E_{LUMO}) \quad (6)$$

$$\eta = \frac{I-A}{2}\ ,\quad \eta = -\frac{1}{2}(E_{HOMO} - E_{LUMO}) \quad (7)$$

Where $I = -E_{HOMO}$ and $A = -E_{LUMO}$ are the ionization potential and electron affinity, respectively.

The fraction of transferred electrons ΔN was calculated according to Pearson theory [22].This parameter evaluates the electronic flow in a reaction of two systems with different electronegativities, in particular case; a metallic surface (Fe) and an inhibitor molecule. ΔN is given as follows:

$$\Delta N = \frac{\chi_{Fe}-\chi_{inh}}{2(\eta_{Fe}+\eta_{inh})} \quad (8)$$

Where χFe and χinh denote the absolute electronegativity of an iron atom (Fe) and the inhibitor molecule, respectively; ηFe and ηinh denote the absolute hardness of Fe atom and the inhibitor molecule, respectively. In order to apply the eq. 8 in the present study, a theoretical value for the electronegativity of bulk iron was used χFe = 7 eV and a global hardness of ηFe = 0, by assuming that for a metallic bulk I = A because they are softer than the neutral metallic atoms [22].

The electrophilicity introduced by Sastri et al [23], is a descriptor of reactivity that allows a quantitative classification of the global electrophilic nature of a compound within a relative scale. They have proposed the ω, as a measure of energy lowering owing to maximal electron flow between donor and acceptor, which defined as follows.

$$\omega = \frac{\chi^2}{2\eta} \quad (9)$$

The Softness σ is defined as the inverse of the η [24]:

$$\sigma = \frac{1}{\eta} \quad (10)$$

3.6. Theoretical study

3.6.1. Quantum chemical calculations

In the last few years, the FMOs (HOMO and LUMO) are widely used for describing chemical reactivity. The HOMO containing electrons, represents the ability (E_{HOMO}) to donate an electron, whereas, LUMO haven't not electrons, as an electron acceptor represents the ability (E_{LUMO}) to obtain an electron. The energy gap

between HOMO and LUMO determines the kinetic stability, chemical reactivity, optical polarizability and chemical hardness–softness of a compound [25].

In this paper, we calculated the HOMO and LUMO orbital energies by using B3LYP method with 6-31G(d,p). All other calculations were performed using the results with some assumptions. The higher values of E_{HOMO} indicate an increase for the electron donor and this means a better inhibitory activity with increasing adsorption of the inhibitor on a metal surface, whereas E_{LUMO} indicates the ability to accept electron of the molecule. The adsorption ability of the inhibitor to the metal surface increases with increasing of E_{HOMO} and decreasing of E_{LUMO}.

High ionization energy (I= 6.67 eV, I= 3.46 eV in gas and aqueous phases respectively) indicates high stability [26-28], the number of electrons transferred (ΔN) was also calculated and tabulated in Table 4. The number of electrons transferred (ΔN) was also calculated and tabulated in Table 5. The ΔN(gas) < 3.6 and ΔN(aqueous) < 3.6 indicates the tendency of a molecule to donate electrons to the metal surface [29, 30].

Table 4. Quantum chemical descriptors of the studied inhibitor at B3LYP/6-31G(d,p) in gas, G and aqueous, A phases

Prameters	Phase	
	Gas	Aqueous
Total Energy *TE* (eV)	-93311.8	-93312.1
E_{HOMO} (eV)	-6.7513	-6.8262
E_{LUMO} (eV)	-0.0952	-0.1771
Gap ΔE (eV)	6.6561	6.6490
Dipole moment μ (Debye)	4.8884	6.1812
Ionisation potential I (eV)	6.7513	6.8262
Electron affinity A	0.0952	0.1771
Electronegativity χ	3.4233	3.5017
Hardness η	3.3281	3.3245
Electrophilicity index ω	1.7606	1.8441
Softness σ	0.3005	0.3008
Fractions of electron transferred ΔN	0.5374	0.5261

The geometry of P2 in gas and aqueous phase (Figure 4) were fully optimized using DFT based on Beck's three parameter exchange functional and Lee–Yang–Parr nonlocal correlation functional (B3LYP) [31] and the 6–31G. The optimized molecular and selected angles, dihedral angles and bond lengths of P P2 are given in figure 4. The optimized structure shows that the molecule P1 and have a non-planar structure. The HOMO and LUMO electrons density distributions of **P2** are given in Table 5.

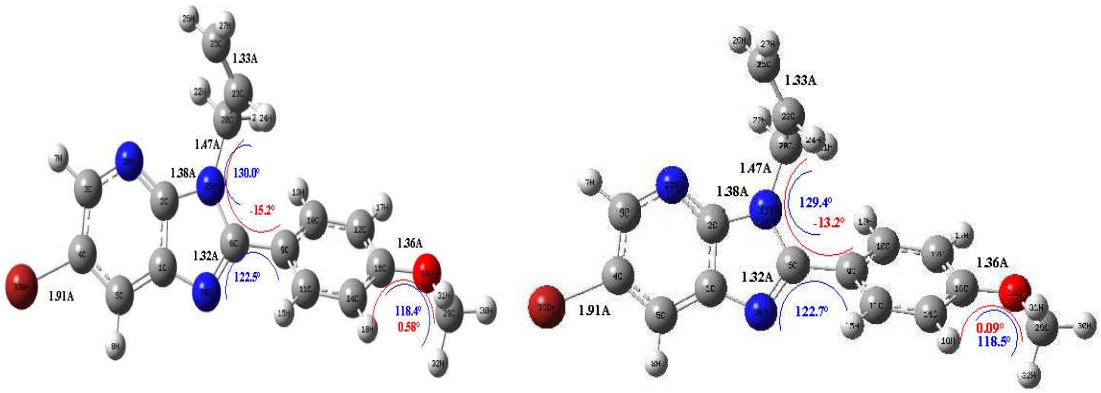

(P2) Gas phase **(P2) Aqueous phase**

Figure 4. Optimized molecular structures and selected dihedral angles (red), angles (blue) and bond lengths (black) of the studied inhibitors calculated in gas and aqueous phase with the DFT at the B3LYP/6-31G level

After the analysis of the theoretical results obtained, we can say that the molecule **P2** have a non-planar structure.

Table 5 : The HOMO and the LUMO electrons density distributions of the studied inhibitors computed at B3LYP/6-31G (d,p) level in gas and aqueous phases

	P2 Gas phase	**P2** Aqueous phase
HOMO	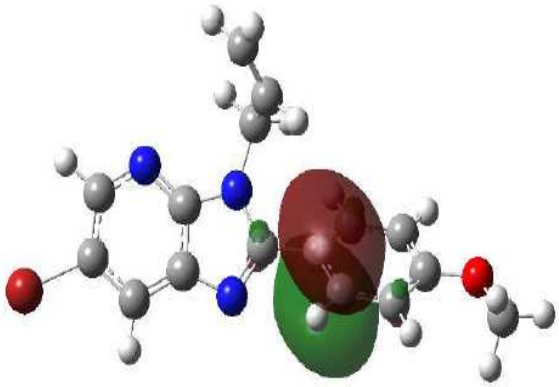	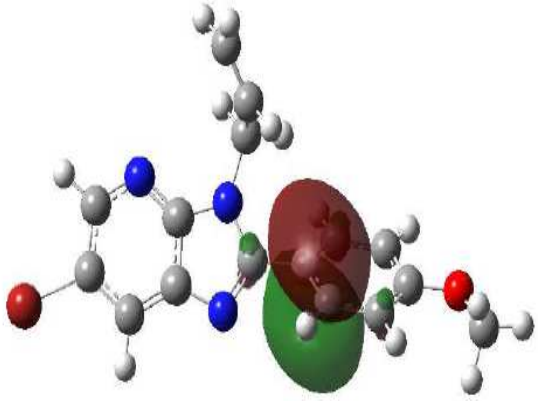
LUMO	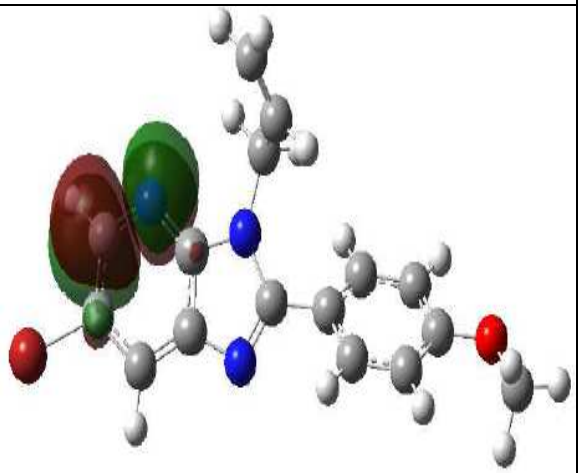	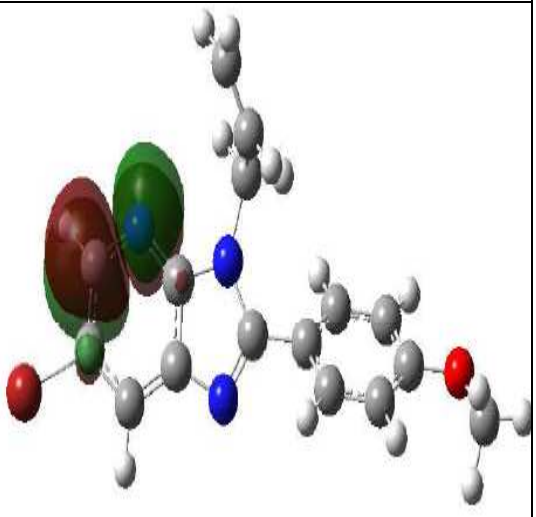

The inhibition efficiency afforded by the quinoline derivative P2 may be attributed to the presence of electron rich O.

CONCLUSION

Based on the results obtained from the experimental and theoretical measurements, the following conclusions are drawn:

- The inhibition efficiency of *P2* on corrosion of mild steel in 1M HCl solution increases on increasing in concentration of P2.
- Potentiodynamic polarization measurement show that it acts as mixed type inhibitor.
- Adsorption of inhibitor molecules of P2 on mild steel surface is found to obey langmuir adsorption isotherm.
- EIS measurement reveals that charge transfer resistance increases with increase in concentration of the P2, indicating that the inhibition increases with increase in concentrations.
- The location of the frontier molecular orbitals (HOMO and LUMO) indicate that P2 may be connected by hydrogen bonds which form ribbon-like infinite sheets and adsorb through the active centers N and O atoms and π electrons.

REFERENCES

[1] N. K. Sebbar, H. Elmsellem, M. Boudalia, S. lahmidi, A. Belleaouchou , A. Guenbour, E. M. Essassi, H. Steli, A. Aouniti, *J. Mater. Environ. Sci*, **2015**, 6 (11), 3034-3044.
[2] H. Elmsellem, H. Nacer, F. Halaimia, A. Aouniti, I. Lakehal, A. Chetouani, S. S. Al-Deyab, I. Warad, R.Touzani, B. Hammouti, *Int. J. Electrochem. Sci*, **2014**, 9, 5328.

[3] Y. Filali Baba, H. Elmsellem, Y. Kandri Rodi, H. Steli, C. AD, Y. Ouzidan, F. Ouazzani Chahdi, N. K. Sebbar, E. M. Essassi, B. Hammouti, *Der Pharma Chemica*, **2016**, 8(4), 159-169.
[4] M. Ellouz, H. Elmsellem, N. K. Sebbar, H. Steli, K. Al Mamari, A. Nadeem, Y. Ouzidan, E. M. Essassi, I. Abdel-Rahaman, P. Hristov, *J. Mater. Environ. Sci*, **2016**,7(7), 2482-2497.
[5] M. Sikine, Y. Kandri Rodi, H. Elmsellem, O. Krim, H. Steli, Y. Ouzidan, A. Kandri Rodi, F. Ouazzani Chahdi, N. K. Sebbar, E. M. Essassi, *J. Mater. Environ. Sci*, **2016**, 7(4), 1386-1395.
[6] M. Y. Hjouji, M. Djedid, H. Elmsellem, Y.Kandri Rodi, Y. Ouzidan, F. Ouazzani Chahdi, N. K. Sebbar, E. M. Essassi, I. Abdel-Rahman, B. Hammouti, *J. Mater. Environ. Sci*, **2016**, 7(4), 1425-1435.
[7] I. Chakib, H. Elmsellem, N. K. Sebbar, S. Lahmidi, A. Nadeem, E. M. Essassi, Y. Ouzidan, I. Abdel-Rahman, F. Bentiss, B. Hammouti., *J. Mater. Environ. Sci*, **2016**, 7(6), 1866-1881.
[8] Y. Filali Baba, H. Elmsellem, Y. Kandri Rodi, H. Steli, F. Ouazzani Chahdi, Y. Ouzidan, N. K. Sebbar, E. M. Essassi, K. Cherrak., *J. Mater. Environ. Sci*, **2016**,7(7), 2424-2434.
[9] K. Tebbji, A. Aouniti, A. Attayibat, B. Hammouti, H. Oudda, M. Benkaddour, S. Radi, A. Nahle, *Indian J. Chem. Technol*, **2011**, 18, 244.
[10] S. El Issami, L. Bazzi, A. Benlhachemi, R. Salghi, B. Hammouti, S. Kertit, *Pigment Resin Tech*, **2007**, 36,161.
[11] K.F. Khaled, N.S. Abdelshafi, A. El-Maghraby, N. Al-Mobarak, *J. Mater. Environ. Sci*, **2011**, 2, 166.
[12] M. Mousavi, M. Mohammadalizadeh, A. Khosravan, *Corros. Sci*, **2011**,53, 3086.
[13] Q. Zhang, G. Zhinong, X. Feng, Z. Xia, *Colloids and Surfaces A: Physicochemical and Engineering Aspects*, **2011**, 380, 191.
[14] H. Elmsellem, M. H. Youssouf, A. Aouniti, T. Ben Hadd, A. Chetouani, B. Hammouti, Russian, *Journal of Applied Chemistry*, **2014**, 87(6), 744−753.
[15] H. Elmsellem, T. Harit, A. Aouniti, F.Malek, A. Chetouani, B.Hammouti, *Protection of Metals and Physical Chemistry of Surfaces, A*, **2015**, 51(5), 873–884.
[16] H.Elmsellem, A.Aouniti, Y. Toubi, H. Steli, M. Elazzouzi, S. Radi, B. Elmahi, Y. El Ouadi, A. Chetouani, B. Hammouti, *Der Pharma Chemica*, **2015**, 7(7), 353-364.
[17] H Elmsellem., H. Bendaha, A. Aouniti, A. Chetouani, M. Mimouni, A. Bouyanzer, *Mor. J. Chem*, **2014**, 2 (1), 1-9.
[18] H. Elmsellem, A. Elyoussfi, H. Steli, N. K. Sebbar, E. M. Essassi, M. Dahmani, Y. El Ouadi, A. Aouniti, B. El Mahi, B. Hammouti, *Der Pharma Chemica*, **2016**, 8(1), 248-256.
[19] A. L. Essaghouani, H. Elmsellem, M. Ellouz, M. El Hafi, M. Boulhaoua, N. K. Sebbar, E. M. Essassi, M. Bouabdellaoui, A. Aouniti and B. Hammouti, *Der Pharma Chemica*, **2016**, 8(2), 297-305.
[20] R.G.Pearson, *Inorg. Chem*, **1988**, 27, 734–740.
[21] H. Elmsellem, N. Basbas, A. Chetouani, A. Aouniti, S. Radi, M. Messali, B. Hammouti, *Portugaliae. Electrochimica. Acta*, **2014**, 2, 77.
[22] H. Elmsellem, H. Nacer, F. Halaimia, A. Aouniti, I. Lakehal, A. Chetouani, S. S. Al-Deyab, I. Warad, R.Touzani, B. Hammouti, *Int. J. Electrochem. Sci*, **2014**, 9, 5328.
[23] I. Lukovits, E. Kalman, F. Zucchi, *Corrosion*, **2001**, 57, 3-7.
[24] H. Elmsellem, A. Aouniti, M. Khoutoul, A. Chetouani, B. Hammouti, N. Benchat, R. Touzani, M. Elazzouzi, *Journal of Chemical and Pharmaceutical Research*, **2014**, 6(4), 1216-1224.
[25] H. Elmsellem, K. Karrouchi, A. Aouniti, B. Hammouti, S. Radi, J. Taoufik, M. Ansar, M. Dahmani, H. Steli, B. El Mahi, *Der Pharma Chemica*, **2015**, 7(10), 237-245.
[26] H. Elmsellem, A. Elyoussfi, N. K. Sebbar, A. Dafali, K. Cherrak, H. Steli, E. M. Essassi, A. Aouniti and B. Hammouti, *Maghr. J. Pure & Appl. Sci*, **2015**, 1, 1-10.
[27] H. Elmsellem, H. Nacer, F. Halaimia, A. Aouniti, I. Lakehal, A. Chetouani, S. S. Al-Deyab, I. Warad, R. Touzani, B. Hammouti, *Int. J. Electrochem. Sci*, **2014**, 9, 5328.
[28] A. Elyoussfi, H. Elmsellem, A. Dafali, K. Cherrak, N. K. Sebbar, A. Zarrouk, E. M. Essassi, A. Aouniti, B. El Mahi and B. Hammouti, *Der Pharma Chemica*, **2015**, 7(10), 284-291.
[29] A. Aouniti, H. Elmsellem, S.Tighadouini, M. Elazzouzi, S. Radi, A. Chetouani, B. Hammouti, A. Zarrouk, *Journal of Taibah University for Science*, **2015**, http://dx.doi.org/10.1016/j.jtusci.2015.11.008.
[30] F. Yousfi, M. El Azzouzi, M. Ramdani, H. Elmsellem, A. Aouniti, N. Saidi, B. El Mahi, A. Chetouani and B. Hammouti, *Der Pharma Chemica*, **2015**, 7(7),377-388.
[31] M. El Azzouzi · A. Aouniti · S. Tighadouin · H Elmsellem · S. Radi ·B. Hammouti · A. El Assyry ·F. Bentiss · A. Zarrouk. DOI: 10.1016/j.molliq.2016.06.007